

Study of radiation damage induced by 24 GeV/c and 26 MeV protons on heavily irradiated MCz and FZ silicon detectors

V. Radicci^{a,*}, L. Borrello^c, M. Boscardin^d, M. Bruzzi^b, D. Creanza^a, G.F. Dalla Betta^c,
M. de Palma^a, E. Focardi^b, A. Macchiolo^b, N. Manna^a, D. Menichelli^b, A. Messineo^c,
C. Piemonte^d, A. Pozza^d, M. Scaringella^b, G. Segneri^c, D. Sentenac^c, N. Zorzi^d

^a*INFN and Dipartimento Interateneo di Fisica, Bari, Italy*

^b*INFN and Università degli Studi di Firenze, Italy*

^c*INFN and Università degli Studi di Pisa, Italy*

^d*ITC-IRST Trento, Povo, Trento, Italy*

^e*Dipartimento di Informatica e Telecomunicazioni Università di Trento, Italy*

Available online 2 October 2006

Abstract

The aim of this work is the development of radiation hard detectors for very high luminosity colliders. A growing interest has been recently focused on Czochralski silicon as a potentially radiation-hard material. We report on the processing and characterization of micro-strip sensors and pad detectors produced by ITC-IRST on n- and p-type magnetic Czochralski and float zone silicon. Part of the samples has been irradiated using 24 GeV/c protons (CERN-Geneva), while another part has been irradiated with 26 MeV protons (FZK-Karlsruhe) up to a fluence of 5×10^{15} 1 MeV-neutron-equivalent/cm². All the samples have been completely characterized before and after irradiation. Their radiation hardness as a function of the irradiation fluence has been established in terms of breakdown voltage, leakage current and evaluating the more relevant mini-sensor parameter variation. Moreover, the time evolution of depletion voltage, leakage current and inter-strip capacitance has been monitored in order to study their annealing behavior and space charge sign inversion effects.

© 2006 Elsevier B.V. All rights reserved.

PACS: 20.40 Gx; 29.40 Wk; 61.82 Fk; 61.80–x

Keywords: Silicon detectors; Radiation damage; Micro-strip detectors

1. Introduction

ATLAS and CMS, two multipurpose high energy physics experiments, are under construction at the Large Hadron Collider (LHC) at CERN. LHC is a large p–p accelerator with a beam energy of 7 TeV and a designed peak luminosity of 10^{34} cm^{−2} s^{−1} [1]. The tracker detectors of both experiments have been designed to work in a very hostile radiation environment with a fast hadron fluence of 3×10^{15} 1 MeV-neutron-equivalent/cm² (n_{eq}/cm^2) expected at the minimum instrumented distance from the collision point (~ 4 cm). Detector technology has been developed to

ensure the survival of these systems to an integrated luminosity of 500 fb^{−1}, corresponding to 10 years of LHC operation [2].

A planned upgrade of the LHC collider (SLHC project [3]) will increase both the luminosity up to a final value of 10^{35} cm^{−2} s^{−1} and the beam energy up to 12.5 TeV. Tracker detectors of SLHC experiments should maintain their performance up to the maximum expected fast hadron fluence: 1.6×10^{16} n_{eq}/cm^2 at 4 cm from the beam line and 8×10^{14} n_{eq}/cm^2 at an intermediate distance of 22 cm. Silicon detectors and in particular micro-strip sensors can still be considered a viable solution in the intermediate and outer tracker regions, provided that an improvement of their radiation hardness to fluences of the order of 10^{15} n_{eq}/cm^2 can be achieved. For this purpose the

*Corresponding author. Tel.: +39 080 544 2432; fax: +39 080 544 2470.
E-mail address: Valeria.Radicci@ba.infn.it (V. Radicci).

activity of the SMART project, a collaboration of Italian research institutes funded by the INFN, has been focused on the development of radiation hard silicon position sensitive detectors for SLHC in the framework of CERN-RD50 collaboration [4].

Previous studies highlighted the beneficial effect in terms of radiation hardness of FZ silicon material enriched with oxygen atoms (DOFZ—diffusion oxygenated FZ silicon) [5]. Nowadays, with the magnetic Czochralski (MCz) growth technology it is possible to produce Si devices with an intrinsically high oxygen content and with a resistivity suitable for particle detector applications [6].

Furthermore, silicon detectors built on p-type substrates (n^+ micro-strip implants on p substrate, i.e., n^+ on p) is a possible radiation harder solution compared to the more common p^+ -on- n technique, mainly for two reasons: first the p substrate, at any dose after irradiation, does not show type inversion, preserving the highest electrical field on the strip side, and second the n^+ implants on p substrate collect electrons which have, with respect to holes, an higher mobility and a lower trapping probability, thus improving charge collection efficiency.

In this paper we report on the results achieved with test structures and micro-strip detectors processed on MCz and FZ substrates (n and p type) heavily irradiated with protons of two different energies.

2. Samples and irradiation campaigns

The wafer processing has been performed by ITC-IRST (Trento, Italy) in two successive runs, using both MCz and FZ 4 inch. silicon wafers for comparison. In the first run (RUN-I) wafers from n -type material have been processed while on the second one (RUN-II) p -type substrates have been manufactured; on both cases the same mask set has been used. For RUN-II the p -spray technique (uniform implantation) [7] is used to obtain isolation between n^+ implants with two different implantation doses, namely $3 \times 10^{12} \text{ cm}^{-2}$ (low p -spray) and $5 \times 10^{12} \text{ cm}^{-2}$ (high p -spray). The wafers produced for RUN-I (p on n) on MCz substrates have a resistivity $\rho \gtrsim 500 \Omega \text{ cm}$, a thickness of $300 \mu\text{m}$ and $\langle 100 \rangle$ crystal orientation, while the ones produced on FZ materials are of type $\langle 111 \rangle$, have a resistivity of around $6 \text{ k}\Omega \text{ cm}$ and a thickness of $300 \mu\text{m}$. For RUN-II (n on p) all the wafers are of $\langle 100 \rangle$ type and have a substrate resistivity $\gtrsim 2 \text{ k}\Omega \text{ cm}$; the thickness is $300 \mu\text{m}$ for MCz substrates and $200 \mu\text{m}$ for FZ silicon.

Each wafer hosts various test structures and ten mini-sensors with equal active area ($\sim 0.5 \times 5 \text{ cm}^2$) but with different geometry, to investigate the dependence of the detector performance on the design parameters (see Table 1). Further details can be found in Refs. [8–10].

The irradiation of the devices was performed with protons of different energies in order to compare the different radiation damages. The first campaign was carried out at the CERN-SPS facility with $24 \text{ GeV}/c$ protons and at fluences up to $3 \times 10^{15} \text{ n}_{\text{eq}}/\text{cm}^2$, the second

Table 1

Strip parameters of the ten mini-sensors in the wafer

μ -strip #	Pitch	Implant width	Poly-width	Al width
S1	50	15	10	23
S2	50	20	15	28
S3	50	25	20	33
S4	50	15	10	19
S5	50	15	10	27
S6	100	15	10	23
S7	100	25	20	33
S8	100	35	30	43
S9	100	25	20	37
S10	100	25	20	41

All the dimensions are in μm . The devices are AC coupled and microstrips are biased through $600 \text{ k}\Omega$ poly-silicon resistors.

one was performed at the Compact Cyclotron of the Forschungszentrum in Karlsruhe (Germany) with 26 MeV protons at fluences up to $2 \times 10^{15} \text{ n}_{\text{eq}}/\text{cm}^2$.

3. Pre-irradiation characterization

All the devices were completely characterized before and after irradiation, following the standard procedures defined within the RD50 Collaboration. The leakage current I_{leak} and the back-plane capacitance C_{back} measurements were performed both on diodes and on micro-strip sensors in order to evaluate the breakdown performance and the depletion voltage. The strip isolation was checked by means of the inter-strip capacitance C_{int} and the inter-strip resistance R_{int} measurements.

Pre irradiation measurements show that all n -type devices (FZ and MCz) show high breakdown voltages ($V_{\text{bd}} > 600 \text{ V}$) and in average all the sensors have a leakage current density around $J \sim 1.4 \text{ nA}/\text{mm}^2$ at 400 V , well beyond their depletion voltage.

Different performance has been observed for p -type sensors that show a low breakdown voltage, in particular for sensors processed with high p -spray dose. Moreover, in detectors with larger pitch ($100 \mu\text{m}$) the breakdown is even lower than 70 V (big dot curves in Fig. 1). A simulation of these devices [11] has identified as responsible for the avalanche breakdown at low bias voltage the high values of the electric field, localized between the n^+ implant and the p -spray layer.

A local variation of the depletion voltage V_{dep} in the MCz material is also measured, especially for p -type wafers, due to the nonuniform oxygen distribution that leads to a spread in the thermal donor activation in the wafer after the processing [10].

For n -type micro-strip sensors a typical behavior of C_{int} as a function of the bias voltage is observed, with a saturation value in over-depletion condition ranging from 0.5 to $1.2 \text{ pF}/\text{cm}$, in agreement with the different device geometries.

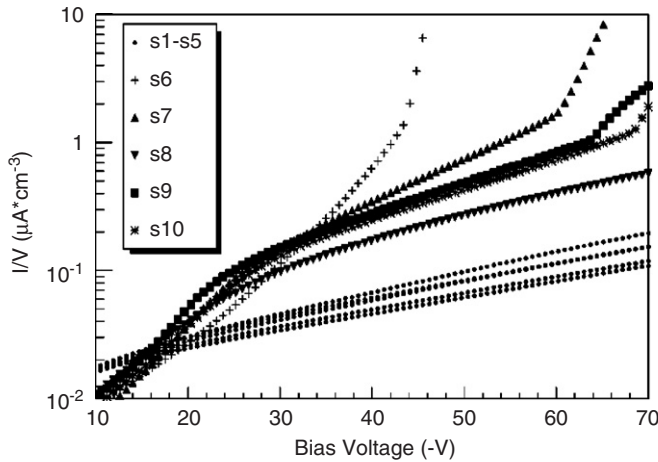


Fig. 1. Leakage currents of MCz p-type, high dose p-spray sensors measured before irradiation. Different curves refer to different geometries, big marks correspond to sensors with 100 μm pitch (s6–s10).

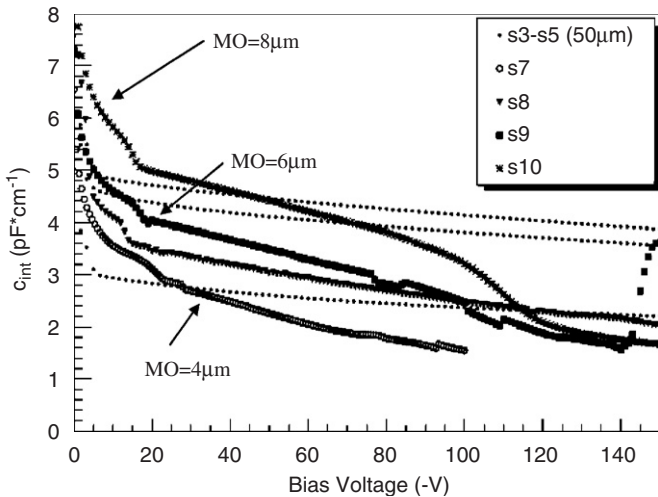


Fig. 2. Inter-strip capacitance of MCz p-type, high dose p-spray sensors measured before irradiation. Different curves refer to different geometries, big marks correspond to sensors with 100 μm pitch (s6–s10).

On the other hand, for p-type sensors the inter-strip capacitance shows a strong variation with bias voltage (Fig. 2) starting from high values at low bias and slowly decreasing to a higher saturation value with respect to n-type sensors, while at the same time the inter-strip resistance is increasing. The C_{int} saturation is faster in sensors processed with low p-spray sensors and for larger pitches. In addition, such behavior is strongly influenced by the metal overhang (Al strip wider than the n^+ strip implant): the coupling between the Al strip and the p-spray layer causes an additional C_{int} contribution that decreases as the bias voltage is increased. This effect is checked by comparing the C_{int} measurements for sensors differing only by the metal overhang extension, see Fig. 2 (sensors s7, s9 and s10 have increasing metal overhang MO).

The effect of the p-spray layer on the strip isolation and the relation between the p-spray dose, the MO and the

inter-strip capacitance are accurately described for different oxide charge densities by device simulations developed at IRST [11]; a good agreement with the experimental data is found.

The simulation results, confirmed by our observations, show that, depending on the oxide charge level and on the MO value, p-spray isolation among n^+ strip implants and optimal inter-strip capacitive coupling C_{int} can be reached, in several cases, only at high bias voltage. This behavior must be carefully followed in irradiated detectors, where it could cause problems if operation in partial depletion conditions were to be requested.

In a few micro-strip sensors CCE has been also measured. The sensors have been assembled in detector units using the CMS front-end electronics and its standard DAQ system [2]. Preliminary measurement show that MCz and FZ n-type detectors have similar performance in terms of collection efficiency and signal to noise value ($S/N \sim 19$) [12].

4. Post-irradiation results

Irradiated devices have been characterized at 0 °C or at –3 °C to reduce the leakage current. All the measurements have been performed immediately after irradiation and after repeated steps during the annealing phase in order to: (i) follow the radiation damage and annealing evolution on bulk current and on effective doping concentration; (ii) determine the effective irradiation fluences; (iii) investigate on space charge sign inversion (SCSI) occurrence for the different materials used (FZ, MCz). It is also interesting to evaluate the scaling factors of the annealing time with the annealing temperature for MCz substrates (the values reported in literature [5] were produced mainly for FZ materials). For this purpose we have performed the annealing of different groups of irradiated samples at different temperatures: 20, 60 or 80 °C. Moreover, by measuring I_{leak} , C_{int} and R_{int} on minisensors at different fluences and annealing times we have studied the radiation hardness of MCz compared to FZ materials, the impact of the geometry (metal overhang, w/p) and, for p-type sensors, of the p-spray dose on the noise level, breakdown voltage and strip isolation.

With the procedure described in Ref. [13,14], the irradiation neutron equivalent fluences are estimated by a fit of the annealing current curves on FZ-n material using the standard parameterisations for the current related damage rate, $\alpha(t, T)$. Subsequently, this factor has been evaluated for all radiation sources on n-type and p-type materials. Measurements have shown a good agreement with NIEL hypothesis; the average damage rate has been estimated: $\langle \alpha \rangle \cong 4 \times 10^{-17} \text{ A/cm}$ after 8 min of annealing at 80 °C, in agreement with expectations [4].

Starting from the diode leakage current we have observed that n-type micro-strip detectors, of both MCz and FZ type, have good performances before and during the annealing treatment, with breakdown voltages well

above V_{dep} . The p-type detectors show an improved performance after irradiation: in the entire fluence range the breakdown voltages of the detectors with a low p-spray dose are fully comparable with the n-type sensors and are in excess of 600 V, although the detectors with high dose p spray recover completely only at irradiation fluences around $6 \times 10^{14} \text{ n}_{\text{eq}}/\text{cm}^2$, as shown in Fig. 3, while for example the breakdown of the detector irradiated at $\Phi_2 = 0.6 \times 10^{14} \text{ n}_{\text{eq}}/\text{cm}^2$ is still $\sim 50 \text{ V}$. This improvement can be explained with the increase, with the irradiation dose, of the positive charge in the passivation oxide layer, which progressively depletes the p spray starting from the interface, bringing a ‘beneficial’ effect in terms of an increased breakdown voltage. This effect is also described and predicted by simulations [11].

The depletion voltage has been measured after irradiation and during the annealing at different temperatures. The annealing behavior of V_{dep} (reported in detail in Refs. [9,12,14]) shows a clear saturation beyond 200 min at 80°C (during the reverse annealing phase) in MCz substrates of both n and p type, while the V_{dep} values of FZ materials still increase with time.

The reduced reverse annealing growth of MCz devices would simplify damage recovery in experimental operational conditions. V_{dep} as a function of fluence is also studied after the beneficial annealing. In n-type material, FZ substrates are already type inverted at the lowest fluence, and V_{dep} increases with fluence ϕ . On the contrary, V_{dep} values of the n-type MCz wafers show a minimum at $\phi_{\text{min}} \sim 1.86 \times 10^{14} \text{ n}_{\text{eq}}/\text{cm}^2$ (Fig. 4). At the minimum the depletion voltage, and, hence, the effective doping concentration N_{eff} is significantly different from zero, suggesting that no SCSI occurred, and that after the minimum the substrate is still n type. However, while MCz devices irradiated at fluences lower than ϕ_{min} show a behavior with annealing time typical of a not yet inverted FZ device

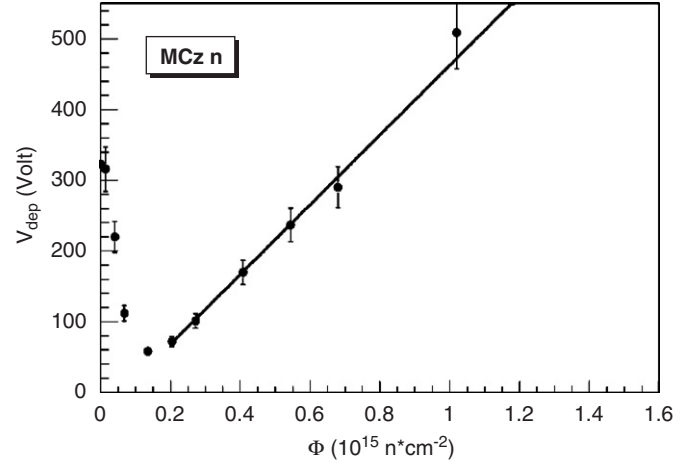


Fig. 4. Depletion voltage vs. fluence for n-type MCz sensors irradiated with 26 MeV protons (see text).

(during the beneficial annealing the depletion voltage leads towards a maximum) the annealing curves of V_{dep} for MCz devices irradiated at fluences higher than ϕ_{min} show a behavior typical of an inverted FZ device (V_{dep} measured during the beneficial annealing leads toward a minimum) [14,15].

Anyway, microscopic investigation by current transients at constant temperature and transient current technique (TCT) measurements have also been performed, giving a different picture: in 24 GeV proton irradiation, n-MCz Si diodes do not exhibit SCSI in the range 10^{14} – $10^{15} \text{ n}_{\text{eq}}/\text{cm}^2$ [15]. Moreover, according to thermally stimulated current (TSC) analysis the deep acceptors produced by irradiation may be partially compensated by a shallow donor, which is introduced with a much higher rate in MCz than in FZ. This observation, if confirmed, could explain a smaller introduction rate of acceptors in MCz and the fact that at $10^{15} \text{ n}_{\text{eq}}/\text{cm}^2$ n-MCz Si is not type inverted. Preliminary simulation studies show that the minimum value of depletion voltage vs. fluence and the ‘inverted like’ annealing behavior without SCSI could be explained in terms of double junction effects [14,15].

In p-type substrates the V_{dep} always increases with irradiation (in fact it still remains p type at any fluence and the acceptor concentration increases with fluence). A lower V_{dep} value is measured at any time and fluences in MCz p-type material with respect to FZ [12].

The MCz and the FZ micro-strip detectors have comparable performances in terms of the inter-strip capacitance C_{int} after irradiation, taking into account that all crystals but n-type FZ (which is $\langle 111 \rangle$) are $\langle 100 \rangle$ oriented. In Figs. 5 and 6 is compared the behavior of C_{int} as a function of bias voltage measured on sensors with the same geometry but different materials and technological production splittings irradiated, respectively, at a low fluence $\phi_2 \sim 0.6 \times 10^{14} \text{ n}_{\text{eq}}/\text{cm}^2$ (sensor geometry S1, $50 \mu\text{m}$) and at a quite high one $\phi_6 \sim 4 \times 10^{14} \text{ n}_{\text{eq}}/\text{cm}^2$ (sensor

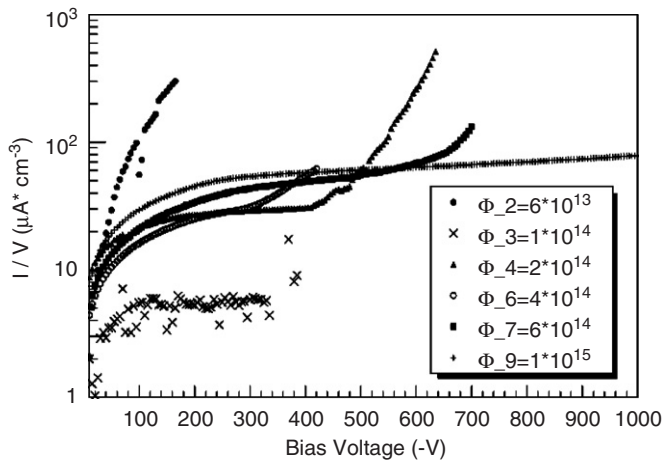


Fig. 3. Leakage Currents of high dose p-spray MCz p-type sensors irradiated with 26 MeV protons at different fluences (from 6×10^{13} to $2 \times 10^{15} \text{ n}_{\text{eq}}/\text{cm}^2$). The measurements are performed at 0°C and rescaled at 20°C .

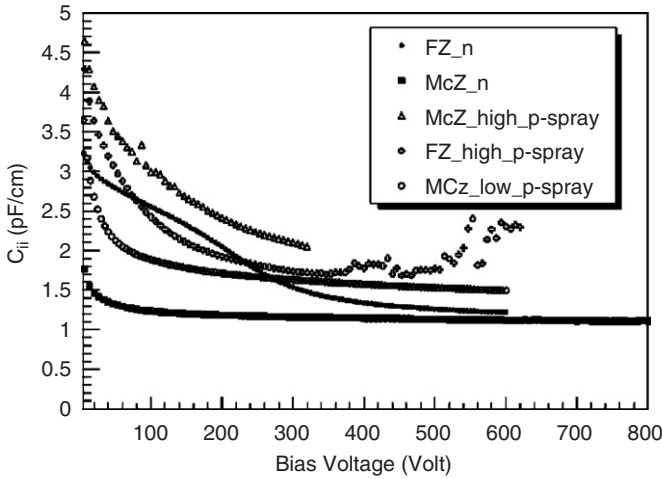


Fig. 5. C_{int} vs. V_{bias} measured on different substrates irradiated with 26 MeV protons at $0.6 \times 10^{14} n_{eq} cm^{-2}$ (sensor geometry s1 with 50 μm pitch).

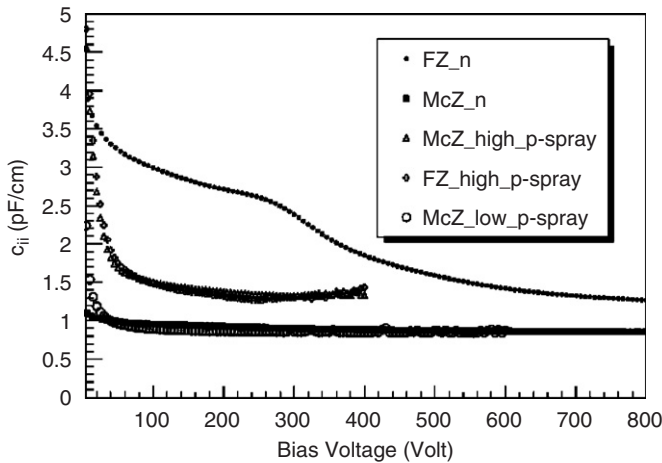


Fig. 6. C_{int} vs. V_{bias} measured on different substrates irradiated with 26 MeV protons at $4 \times 10^{14} n_{eq} cm^{-2}$ (sensor geometry s6 with 100 μm pitch).

geometry S6, 100 μm). For the n-type detectors (full markers) C_{int} is not varying significantly with the fluence, with the FZ devices following the classical $\langle 111 \rangle$ behavior [16]. The post-irradiation value for MCz sensors, after a sharp initial decrease with V_{bias} is slightly higher and in the same range of the pre-irradiation values: 1.2–1.7 pF/cm for the detectors with a strip pitch of 50 μm and 0.5–1 pF/cm for the 100 μm pitch sensors.

For what concerns p-type detectors (empty markers), the same features observed before irradiation in the C_{int} vs. V_{bias} curves are still present: inter-strip capacitance decreases with V_{bias} towards a saturation value. The saturation is still faster for low p-spray isolation and for larger pitches. It can be observed that the C_{int} behavior for p-type devices improves with irradiation; in particular, low p-spray sensors show pretty comparable behavior to n-type MCz irradiated sensors starting from $\phi_3 \sim 1 \times 10^{14} n_{eq}/cm^2$

[14] while the high p-spray curves are still higher at $\phi_6 \sim 4 \times 10^{14} n_{eq}/cm^2$ (Fig. 6). No differences between FZ and MCz substrates have been observed (in Fig. 6 FZ and MCz high p-spray curves are quite similar). The improvement of p-type micro-strip sensor performances for what concerns breakdown voltage and inter-strip capacitance is also nicely predicted by device simulation [11], where it is explained in terms of oxide charge density for different p-spray dose choices.

5. Conclusion

In this work we have summarized some of the results achieved within the SMART collaboration on the characterization of heavily irradiated silicon devices. Before and after irradiation with protons up to $3 \times 10^{15} n_{eq}/cm^2$, n-type and p-type MCz Si micro-strip detectors were qualified in comparison with standard FZ substrates. We have observed an improved radiation tolerance of MCz detectors with respect to standard FZ ones in terms of depletion voltage as a function of fluence and especially during the reverse annealing phase. A very good behavior has been observed in terms of inter-strip capacitance after irradiation of n-type materials. Both the low breakdown voltage and the high inter-strip capacitance values, observed on p-type unirradiated substrates, recover with the irradiation doses up to the maximum one investigated. Simulation studies are ongoing in order to optimize the p-spray dose and investigate other strip isolation technique (p-stop, moderate p-spray [11]). These first results support the possible use of MCz n-type and p-type devices as a cost-effective solution in the intermediate and outer layers of the SLHC tracker detectors.

References

- [1] LHC collaboration, The Large Hadron Collider, conceptual design, CERN/AC/95-05.
- [2] CMS Collaboration, The Tracker project, Technical Design Report, CERN/LHCC 1998-006, Addendum to the CMS Tracker TDR, CERN/LHCC 2000-016.
- [3] F. Gianotti, et al., Eur. Phys. J. C 39 (2005) 293.
- [4] RD50 Collaboration, Status reports, <http://rd50.web.cern.ch/rd50/>.
- [5] M. Moll, Radiation damage in silicon particle detectors—microscopic defects and macroscopic properties, DESY-THESIS/1999/040.
- [6] V. Savolainen, et al., J. Cryst. Growth 243 (2) (2002).
- [7] R.H. Richter, et al., Nucl. Instr. and Meth. A 377 (1996) 412.
- [8] M. Bruzzi, et al., Nucl. Instr. and Meth. A 552 (2005) 20.
- [9] A. Macchiolo, et al., Characterization of micro-strip detectors made with high resistivity n- and p-type Czochralski silicon, in: Proceedings of the PSD07 Conference, Nucl. Instr. and Meth. A, submitted for publication (to be published).
- [10] C. Piemonte, Preliminary electrical characterization of n-on-p devices fabricated at ITC-irst, in: Proceedings of the Fifth RD50 Workshop, available: <http://rd50.web.cern.ch/rd50/>.
- [11] C. Piemonte, TCAD simulations of isolation structures for n⁺-on-p silicon microstrip detectors, in: Proceedings of the Seventh RD50 Workshop, available: <http://rd50.web.cern.ch/rd50/>.
- [12] A. Messineo, et al., Development of radiation hard silicon detectors: the SMART project, in: Proceedings of the 9th Conference on

- Astroparticle, Particle and Space Physics, Detectors and Medical Applications, World Scientific 2005, ISBN 981-256-798-4.
- [13] D. Creanza, et al., Nucl. Instr. Meth. A 485 (2002) 109.
- [14] G. Segneri, et al, Radiation hardness of high resistivity n- and p-type magnetic Czochralski silicon, in: Proceedings of the PSD07 conference, Nucl. Instr. and Meth. A, submitted for publication (to be published).
- [15] M. Scaringella, et al., in: Proceedings of the Seventh International Conference on Large Scale Applications and Radiation Hardness of Semiconductor Detectors, Nucl. Instr. and Meth. A, submitted for publication.
- [16] RD50 Collaboration, Status Reports 2005, <http://rd50.web.cern.ch/rd50/>.